Is Lung Ultrasound Imaging a Worthwhile Procedure for Severe Acute Respiratory Syndrome Coronavirus 2 Pneumonia Detection?

Giovanni Battista Fonsi, MD, PhD, Paolo Sapienza, MD, PhD, Gioia Brachini, MD, PhD, Chiara Andreoli, MD, Maria Luisa De Cicco, MD, Bruno Cirillo, MD, Simona Meneghini, MD, Francesco Pugliese, MD, Daniele Crocetti, MD, Enrico Fiori, MD, Andrea Mingoli, MD (iD)

Address correspondence to Andrea Mingoli, MD, Department of Surgery, Sapienza University of Rome, Policlinico Umberto I, Viale del Policlinico 155, 00161 Rome, Italy.

E-mail: andrea.mingoli@uniroma1.it

Abbreviations

AUC, area under the curve; CI, confidence interval; COVID-19, coronavirus disease 2019; CT, computed tomography; GGO, ground glass opacity; IQR, interquartile range; LR, likelihood ratio; LUS, lung ultrasound; NPV, negative predictive value; PPV, positive predictive value; ROC, receiver operating characteristic; rRT-PCR, real-time reverse transcriptase polymerase chain reaction; SARS-CoV-2, severe acute respiratory syndrome coronavirus 2; US, ultrasound

Objectives—We compared 2 imaging modalities in patients suspected of having coronavirus disease 2019 (COVID-19) pneumonia. Blinded to the results of real-time reverse transcriptase polymerase chain reaction (rRT-PCR) testing, lung ultrasound (LUS) examinations and chest computed tomography (CT) were performed, and the specific characteristics of these imaging studies were assessed.

Methods—From March 15, 2020, to April 15, 2020, 63 consecutive patients were enrolled in this prospective pilot study. All patients underwent hematochemical tests, LUS examinations, chest CT, and confirmatory rRT-PCR. The diagnostic performance of LUS and chest CT was calculated with rRT-PCR as a reference. The interobserver agreement of radiologists and ultrasound examiners was calculated. Ultrasound and CT features were compared to assess the sensitivity, specificity, positive predictive value, and negative predictive value. Positive and negative likelihood ratios measured the diagnostic accuracy.

Results—Nineteen (30%) patients were COVID-19 negative, and 44 (70%) were positive. No differences in demographics and clinical data at presentation were observed among positive and negative patients. Interobserver agreement for CT had a κ value of 0.877, whereas for LUS, it was 0.714. The sensitivity, specificity, positive predictive value, and negative predictive value of chest CT for COVID-19 pneumonia were 93%, 90%, 85%, and 95%, respectively; whereas for LUS, they were 68%, 79%, 88%, and 52%. On receiver operating characteristic curves, area under the curve values were 0.834 (95% confidence interval, 0.711–0.958) and 0.745 (95% confidence interval, 0.606–0.884) for chest CT and LUS.

Conclusions—Lung ultrasound had good reliability compared to chest CT. Therefore, our results indicate that LUS may be used to assess patients suspected of having COVID-19 pneumonia.

Key Words—chest computed tomography; coronavirus disease 2019; lung ultrasound; severe acute respiratory syndrome coronavirus 2

S ince December 2019, novel coronavirus disease 2019 (COVID-19) has rapidly spread all over the world, causing extremely high mortality in several countries (United States, Brazil, United Kingdom, Italy, and France), globally assessed at

more than 506,000 deaths at the end of June 2020 and also a catastrophic increase in hospital care expenditures because of the implementation of supportive facilities. Most patients infected by severe acute respiratory syndrome coronavirus 2 (SARS-CoV-2) are completely asymptomatic or develop mild respiratory and constitutional symptoms,[1] thus conferring a high risk of infection of other noninfected populations.

Specific lung abnormalities may develop even before clinical manifestations (elevation in body temperature > 37.5°C and cough); therefore, a confirmatory real-time reverse transcriptase polymerase chain reaction (rRT-PCR) examination and early chest computed tomography (CT) have been proposed.[2] Fang et al[3] demonstrated that the sensitivity of chest CT was greater than that of rRT-PCR (98% versus 71%, respectively; P < .001) in identifying SARS-CoV-2 infection. In fact, a low viral load or improper sampling negatively influences the results of rRT-PCR. More recently, Long et al[2] also confirmed the superiority of chest CT over rRT-PCR, with sensitivity of 97.2% versus 84.6%, in the initial diagnosis of COVID-19 pneumonia. However, the costs, exposure to radiation, high contagiousness of SARS-CoV-2, and risk of in-hospital disease spreading make chest CT a limited option to rapidly diagnose and follow the course of the pneumonia.[4] Over the past years, lung ultrasound (LUS) has evolved considerably, greatly expanding its clinical application; therefore, it might give theoretically similar results as chest CT and superior results over standard radiography, having the advantages of being usable at the point of care, repeatable, being free of radiation exposure, and last but not least, not affecting hospital expenditures because of its low cost.

To our knowledge, no studies to date have investigated the role of LUS in the detection of pulmonary infection sustained by SARS-CoV-2, and no data on the specificity, sensitivity, positive predictive value (PPV), negative predictive value (NPV), and diagnostic accuracy are available. In this study we compared 2 imaging modalities in patients suspected of having COVID-19 pneumonia. Blinded to the results of rRT-PCR testing, LUS examinations and chest CT were performed, and the specific characteristics of these imaging studies were assessed.

Materials and Methods

Study Setting and Design
This prospective pilot study was conducted in the Policlinico Umberto I hospital, located at the border of the historical center of the city, which is 1 of the 3 affiliated hospitals of the Sapienza University and 1 of the 5 referring hospitals for emergencies and trauma in the Lazio region. After completing a prescreening questionnaire about COVID-19 symptoms in a dedicated area of the emergency department, all consecutive patients emergently admitted from March 15, 2020, to April 15, 2020 and affected with fever higher than 37.5°C, cough, dyspnea, or a combination thereof who underwent hematochemical and arterial blood gas tests, LUS examinations, thin-section chest CT, and confirmatory rRT-PCR examinations formed the basis of the study. Demographic data and information on symptoms at presentation (classified as mild, moderate, or severe[5]), comorbidities, laboratory results, and outcomes were collected. We excluded patients transferred to another hospital or lost to follow-up.

Patient data were collected according to the principles laid down in the Declaration of Helsinki, and formal ethical approval from our Institutional Research Committee (Department of Surgery Pietro Valdoni) was obtained. Written informed consent for treatment and the analysis of data for scientific purposes was obtained from all patients.

Sample Size
Since no exhaustive literature is available on the comparison between LUS and chest CT for the diagnosis of COVID-19–positive patients, the preliminary definition of the sample size was not quantifiable, but we expected to collect at least 60 patients.

Chest CT
Computed tomographic examinations were performed, within the first 2 hours of admission and before rRT-PCR results, on a 64-slice scanner (Somatom Sensation; Siemens Medical Solutions, Forchheim, Germany) dedicated only to patients with COVID-19. The scanning parameters were as follows: tube voltage, 140 kV; tube current modulation, 100 mAs; spiral pitch factor, 1.5; and collimation, 0.6 mm. Images were reconstructed with a 1-mm slice

thickness using a high-frequency reconstruction algorithm. Decontamination of the room consisted of surface disinfection with 62% to 71% ethanol or 0.1% sodium hypochlorite. After each patient's chest CT examination, passive air exchange was performed for 40 to 60 minutes. Acquisitions were performed with the patient laying down and the arms raised during a deep-inspiration breath hold, without contrast agent administration. Blinded to rRT-PCR results, 2 radiologists (C.A. and M.L.D.C.), who were experienced in chest imaging, studied all chest CT images. In cases of disagreement, a consensus was reached. The CT evaluation included the following features[6]: (1) ground glass opacities (GGOs); (2) consolidation; (3) a mixed GGO and consolidation pattern; (4) single or multiple solid nodules surrounded by GGOs (halo sign); (5) a focal or multifocal distribution; (6) GGO and consolidation location (upper, middle, or lower lobe); (7) multilobe involvement; (8) a bilateral distribution; (9) interlobular septal thickening; (10) an air bronchogram; (11) the presence of cavitation; (12) bronchial wall thickening; (13) bronchiectasis; (14) mediastinal lymph node enlargement (defined as a lymph node with a short axis > 10 mm); (15) pleural effusion; and (16) pericardial effusion.

Lung Ultrasound
Patient Position
The examiner scanned the anterior, lateral, and posterior areas of the thorax, and the whole pulmonary area was covered from the basal to the upper quadrants of the thorax. Four vertical lines in each hemithorax (right parasternal line, right anterior-axillary line, right posterior-axillary line, right paravertebral line, left parasternal line, left anterior-axillary line, left posterior-axillary line, and left paravertebral line) were followed to perform a systematic examination with the patients placed in both supine and lateral positions.

Technique
Lung ultrasound examinations were performed, within the first 2 hours of admission and before rRT-PCR results, by 2 examiners (G.B.F. and G.B.), who were experienced in echography and blinded to rRT-PCR results, using convex and linear vascular transducers (2.5–5 and 7.5–12 MHz, respectively) connected to a portable echograph (MyLab 25 Gold;

Esaote SpA, Genoa, Italy). The risk of contagion for the operator and contamination of the device with an eventual hospital spread was decreased by respecting all the preventive measures for respiratory, droplet, and contact isolation provided by the World Health Organization for the SARS-CoV-2 infection. Lung ultrasound studies were performed in a dedicated room, and at the end of the procedure, the portable echograph with the connected transducer was sterilized in a dedicated area and put into 2 new sterile plastic bags.

Acquisition Protocol
We performed LUS examinations using the 12-zone method.[7] Scans of the 3 different areas of each hemithorax (anterior, lateral, and posterior) and superior and inferior segments were performed (Figure 1). Therefore, 6 specific regions for each lung were scanned per patient for 60 seconds. Scans needed to be intercostal to cover the widest surface possible with a single scan. Lung ultrasound included the following features: (1) a thickened pleural line with a pleural line irregularity; (2) A-lines; (3) B-lines (≥3 nonconfluent or confluent); (4) consolidations; (5) B-line and consolidation location (upper, middle, or lower lobe); (6) multilobe involvement; (7) a bilateral distribution; (8) an air bronchogram; (9) pleural effusion; and (10) pericardial effusion.

Chest CT Features Not Detectable With LUS
The following chest CT features were not detectable with LUS because of the intrinsic limit of this diagnostic tool: halo sign, interlobular septal thickening, the presence of cavitation, bronchial wall thickening, bronchiectasis, and mediastinal lymph node enlargement.

Real-time RT-PCR
Nasopharyngeal and oropharyngeal swabs were obtained for each patient to assess the positivity or negativity for SARS-COV2 with rRT-PCR.[8] The rRT-PCR results served as the reference standard. All patients received 2 nasopharyngeal and oropharyngeal swabs at an interval of 24 hours. Patients were considered positive after 2 consecutive positive rRT-PCR results. According to the rRT-PCR results, the patients were divided in COVID-19 positive and negative.

Figure 1. Schematic representation of the 6 acquisition areas on each hemithorax with the patient supine and in a lateral position: anterior-superior (yellow), lateral-superior (beige), posterior-superior (orange), anterior-inferior (green), lateral-inferior (pink), and posterior-inferior (blue). Anatomic landmarks are indicated.
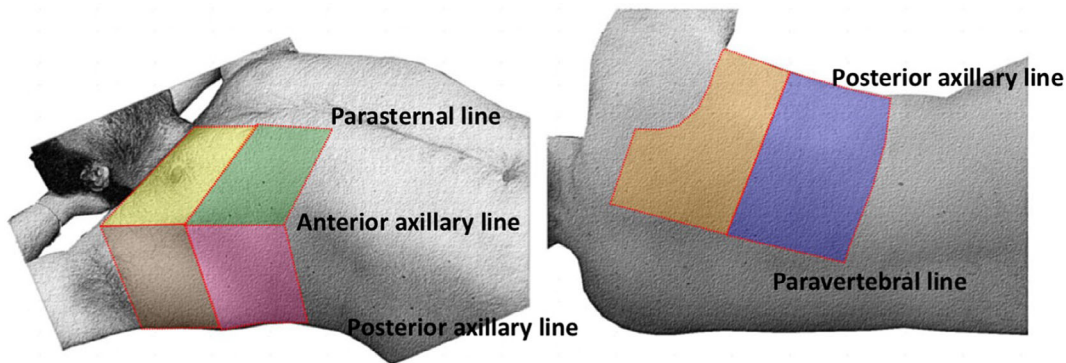
Statistical Analysis

Data were analyzed with SPSS version 25.0.0.2 software (IBM Corporation, Armonk, NY). Nonparametric tests were used because of the sample sizes. The Mann–Whitney U test was used to analyze the continuous variables, whereas the χ^2 test or Fisher exact test was used for the categorical variables. Data are expressed as the mean $\pm$ standard deviation, median, interquartile range (IQR), and mode because of the heterogeneity of the sample. Correlations between symptoms at presentation and chest CT and LUS results were calculated by the bivariate Spearman method. The interobserver agreement of radiologists and ultrasound (US) examiners was calculated. A κ value of 1.000 indicated perfect agreement, a κ value of 0.000 no agreement, and a κ value of -1.000 complete disagreement. Therefore, for the purpose of this study, we considered that a κ value greater than 0.7 implied acceptable agreement, a κ value greater than 0.8 good agreement, and a κ value greater than 0.9 excellent agreement.[9,10] The sensitivity, specificity, PPV, and NPV with rRT-PCR as the reference standard were calculated between chest CT and LUS. Positive and negative likelihood ratios (LRs) measured the diagnostic accuracy. Positive and negative LRs were defined a good/excellent when greater than 7 and less than 0.5, respectively. The CT and US features were used to estimate nonparametric receiver operating characteristic (ROC) curves and the area under the curve (AUC) reflecting the predictive value of chest CT and LUS. Area under the curve values between 0.8 and 1.0 were considered very good/excellent, 0.6 to 0.8 sufficient/good, and from less than 0.5 to 0.6 insufficient. The 95% confidence interval (CI) was reported when appropriate. Differences with $\alpha < .05$ were considered statistically significant.

Results

Patient Characteristics and Clinical Data

Overall, there were 63 patients (41 male and 22 female; mean age, 63 ± 14 years; median, 65 years; mode, 78 years; IQR, 25 years; and range, 35–91 years). No patients presented with mild symptoms, but 46 (73%) patients had moderate and 17 (27%) had severe symptoms. Nineteen (30%) COVID-19–negative patients were affected by bacterial (4 patients) or viral (7 patients) pneumonia, exacerbation of chronic obstructive pulmonary disease (6 patients), and acute respiratory distress syndrome due to pancreatitis (1 patient) and uremia (1 patient). Forty-four (70%) were COVID-19 positive. All patients presented with fever higher than 37.5°C, whereas cough was present in 33 (52%) and dyspnea in 35 (55%). The time from symptoms onset to hospitalization ranged from 1 to 12 days (mean, 5 ± 3 days; median, 5 days; mode, 3 days; and IQR, 3 days); 49 (78%) patients presented from 1 to 7 days after the onset of symptoms and the remaining 14 (22%) after the first week. Hematochemical blood tests at admission showed a mean lymphocyte count of $0.9 \pm 0.5 \times 10^9$/L (range, 0.2–2.5×10^9/L; median, 0.8×10^9/L; mode, 0.7×10^9/L; and IQR, 0.6×10^9/L). Lymphocytopenia (defined as a lymphocyte count $<1 \times 10^9$/L) was recorded in

Table 1. Demographics, Clinical Data, and Hematochemical Test Results of the Groups of Patients

Parameter	COVID-19– (n = 19)	COVID-19+ (n = 44)	P
Male/female	12/7	29/15	.783
Age, y	61 ± 15	66 ± 13	.489
Symptoms at presentation			.115
Moderate	17 (89)	38 (86)	
Severe	2 (10)	6 (14)	
Fever,°C	38 ± 0.5	38 ± 0.8	.697
Symptom onset, d	5.4 ± 3.4	5.2 ± 2.9	.818
Hematochemical tests			
Lymphocyte count, ×10^9/L	0.93 ± 0.25	0.89 ± 0.55	.761
High-sensitive C-reactive protein, mg/dL	9 ± 12	12 ± 11	.883
Arterial oxygen saturation, %	97 ± 1	95 ± 6	.924

Data are presented as mean ± SD and number (percent) where applicable.

39 (62%) patients. The mean high-sensitive C-reactive protein level was 12 ± 14 mg/L (range, 0.2–54 mg/L; median, 6 mg/L; mode, 3 mg/L; and IQR, 13 mg/L). An elevated high-sensitive C-reactive protein level (defined >10 mg/L) was observed in 24 (38%) patients. Arterial blood gas tests at admission showed mean arterial oxygen saturation of 96% ± 5% (range, 70%–100%; median, 97%; mode, 98%; and IQR, 4%). Eleven (17%) patients were hypoxemic (defined as arterial oxygen saturation < 90%)

at admission. There were no statistical differences in demographics, clinical data, and hematochemical test results at presentation among COVID-19–negative and COVID-19–positive patients (Table 1).

Outcomes

Fourteen (22%) patients were hospitalized in the intensive care unit (10 COVID-19–positive and 4 COVID-19–negative patients) and required invasive mechanical ventilation. The remaining COVID-

**Table 2.** Chest CT Features of the Groups of Patients

Feature	COVID-19–(n = 19)	COVID-19 + (n = 44)	P
GGOs	2 (10)	10 (23)	.318
Consolidation	0 (0)	5 (11)	.311
Mixed GGOs and consolidation	2 (10)	28 (64)	.001
Halo sign	0 (0)	4 (9)	.306
Abnormalities			.001
Focal	18 (95)	23 (52)	
Multifocal	1 (5)	21 (48)	
GGO and consolidation location			.001
Upper lobe	10 (53)	1 (2)	
Middle lobe[a]	3 (16)	6 (14)	
Lower lobe	6 (31)	37 (84)	
Multilobe involvement	2 (10)	42 (95)	.001
Bilateral distribution	2 (10)	42 (95)	.001
Interlobular septal thickening	2 (10)	34 (77)	.001
Air bronchogram	2 (10)	15 (34)	.047
Presence of cavitation	0 (0)	3 (7)	.334
Bronchial wall thickening	2 (10)	27 (61)	.001
Bronchiectasis	0 (0)	11 (25)	.025
Mediastinal lymph node enlargement	0 (0)	23 (52)	.001
Pleural effusion	2 (10)	10 (23)	.318
Pericardial effusion	0 (0)	4 (9)	.306

Data are presented as number (percent).
[a]The middle lobe was counted only for the right side.

Figure 2. A and **B**, Chest CT shows bilateral GGOs with a peripheral subpleural distribution in the upper lobes of both lungs. **C** and **D**, Chest CT shows large peripheral subpleural bilateral GGOs without a consolidation area or pleural effusion.
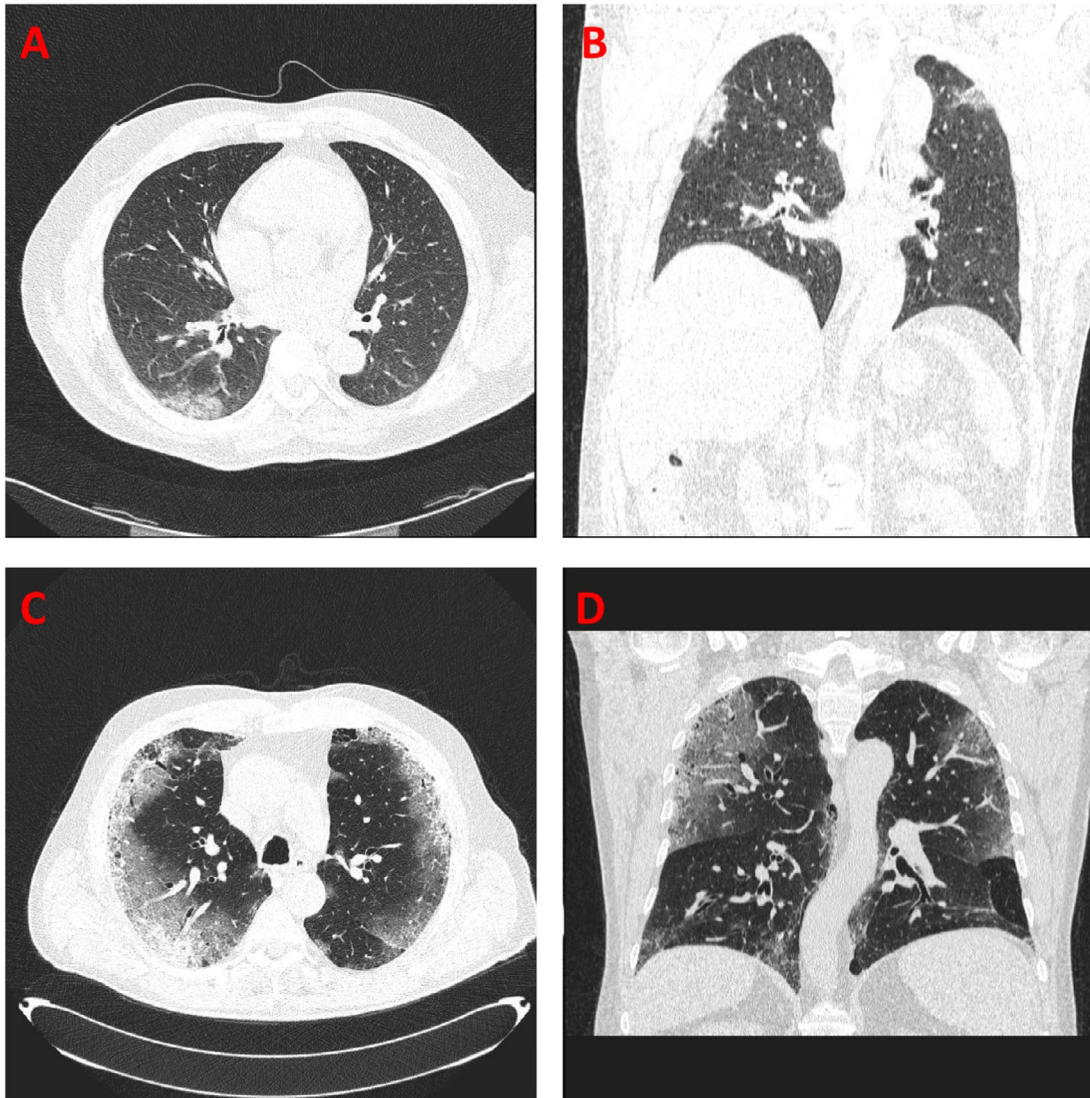
19–positive patients were hospitalized in a dedicated area of the hospital receiving noninvasive respiratory support. Overall, 5 (8%) patients died: 4 COVID-19–positive patients for pulmonary complications and 1 COVID-19–negative patient for cardiac and kidney complications. Fifty-eight (92%) patients were discharged alive from the hospital. The mean hospital stay was 36 ± 14 days (range, 11–61 days; median, 37 days; mode, 31 days; and IQR, 20 days). COVID-19–positive patients were hospitalized for a longer period (mean, 40 ± 13 days) compared to COVID-19–negative patients (mean, 27 ± 10 days; $P = .001$; 95% CI, -19.524–-7.318).

Correlations Between Symptoms at Presentation, Chest CT, and LUS

We found a significant correlation between chest CT and symptoms at presentation ($\rho = .405$; $P = .038$) as well as with LUS ($\rho = .384$; $P = .045$).

Chest CT Findings

Detailed results of chest CT findings are reported in Table 2. Briefly, a mixed GGO and consolidation

pattern with a bilateral distribution, multifocal abnormalities, and multilobe involvement, in association with interlobular septal thickening, an air bronchogram, bronchial wall thickening, and mediastinal lymph node enlargement were significantly present in COVID-19–positive patients compared to COVID-19–negative patients (Figure 2, A and B).

Lung Ultrasound Findings
The results are described in Table 3. Briefly, at LUS, COVID-19–positive patients had a significantly higher presence of various B-line patterns (≥ 3 confluent or nonconfluent) due to interlobular septa thickening or areas of consolidation often obscuring the underlying bronchial structures or pulmonary parenchyma, with a multilobe and bilateral distribution compared to COVID-19–negative patients (Figure 3).

Interobserver Agreement for CT and LUS
Interobserver agreement for CT was good, with a κ value of 0.877 for the radiologists. They disagreed for 3 (6%) results. Interobserver agreement for US was acceptable, with a κ value of 0.714 for the US examiners. They disagreed for 8 (12%) results.

Diagnostic Performance of CT
The sensitivity, specificity, PPV, and NPV of CT for COVID-19 pneumonia were 93%, 90%, 85%, and 95%, respectively. Positive and negative LRs were

8.85 (95% CI, 2.38–33) and 0.08 (95% CI, 0.03–0.23). The ROC curve is reported in Figure 4A. The AUC was 0.834 (95% CI, 9.711–0.958).

Diagnostic Performance of LUS
The sensitivity, specificity, PPV, and NPV of LUS for COVID-19 pneumonia were 68%, 79%, 88%, and 52%, respectively. Positive and negative LRs were 2.33 (95% CI, 1.44–3.78) and 0.33 (95% CI, 0.14–0.81). The ROC curve is reported in Figure 4B. The AUC was 0.745 (95% CI, 0.606–0.884).

Discussion

In Italy, the spread of SARS-CoV-2 has represented a major problem because of overwhelming transmission, and the severity of the disease and has caused, especially in some areas in the north of Italy, a threat for the national health care system because of the limited availability of hospital resources (ie, intensive care units and facilities) and medical and paramedical personnel. During the next fall season, the pandemic might have a resurgence; thus, the health system and the personnel should be well aware to reduce the risk of contagion spread.

At present, chest CT is considered the reference standard to diagnose COVID-19 pneumonia, especially in an emergency setting where rapid
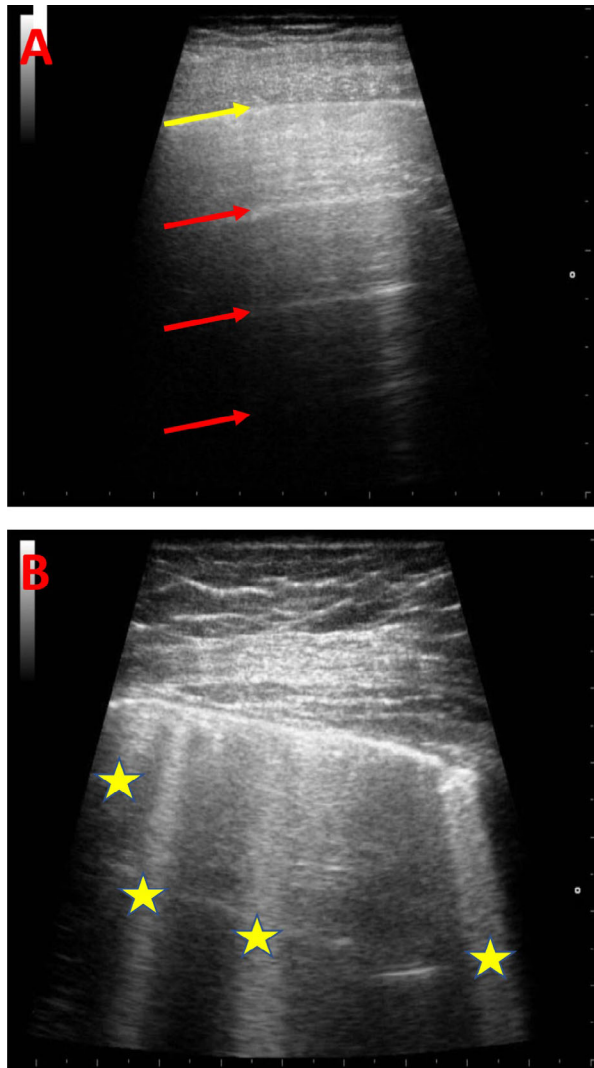
Table 3. Lung Ultrasound Features of the Groups of Patients

Feature	COVID-19–(n = 19)	COVID-19 + (n = 44)	P
Thickened pleural line	4 (21)	38 (86)	.001
A-line	10 (53)	9 (20)	.017
B-line			.001
≤2 nonconfluent or confluent	19 (100)	9 (20)	
≥3 nonconfluent or confluent	0 (0)	35 (80)	
Consolidation	2 (10)	20 (45)	.009
B-line and consolidation location			.018
Upper lobe	9 (48)	7 (16)	
Middle lobe[a]	8 (42)	6 (14)	
Lower lobe	2 (10)	31 (70)	
Multilobe involvement	6 (32)	34 (77)	.001
Bilateral distribution	2 (10)	33 (75)	.001
Air bronchogram	4 (21)	17 (39)	.247
Pleural effusion	1 (5)	8 (18)	.256
Pericardial effusion	0 (0)	0 (0)	NA

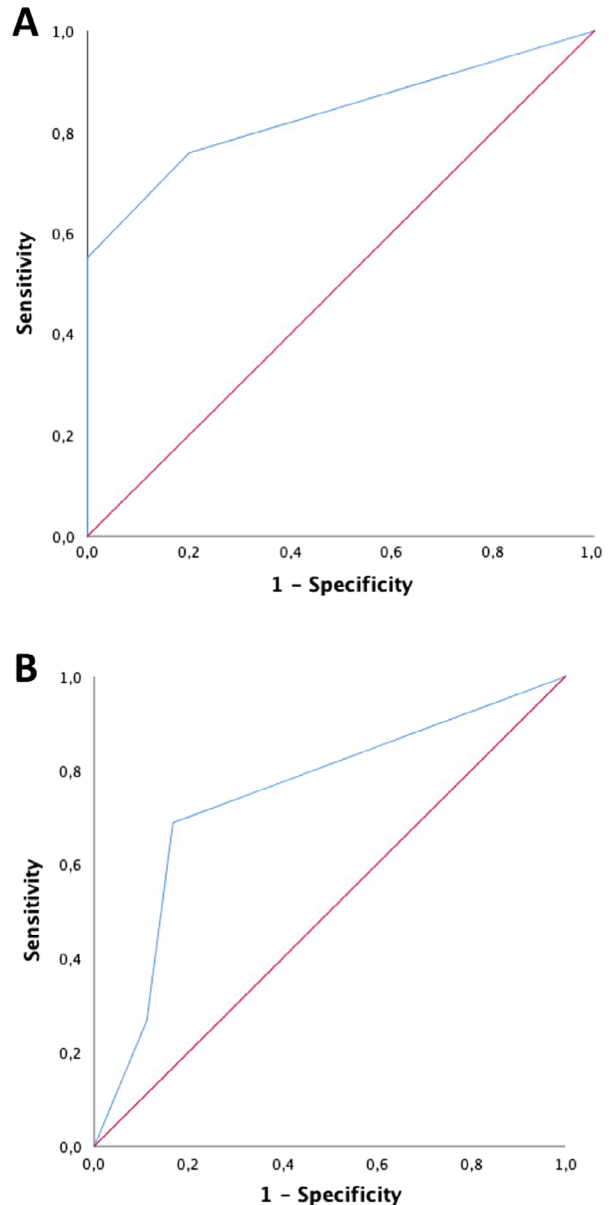Data are presented as number (percent). NA indicates not applicable.
[a]The middle lobe was counted only for the right side.

Figure 3. A, Lung ultrasound image from a COVID-19–negative patient. A-lines (yellow arrow) are visible, which are a repetition of the pleural line (red arrows) at the same distance from the skin to the pleural line, thus indicating the presence of air below the pleural line (corresponding to the parietal pleura). A-lines can be complete or partial (as shown here). **B**, Typical LUS image of SARS-CoV-2 pneumonia, characterized by the presence of several B-lines (asterisks). B-lines are hyperechoic laserlike artifacts resembling the tail of a comet, which arise from the pleural line and move together with the lung sliding. A-lines are abolished because of the presence of B-lines.

Figure 4. A, Nonparametric ROC curve and the AUC reflecting the predictive value of chest CT. The AUC was 0.834 (95% CI, 0.711–0.958). **B**, Nonparametric ROC curve and the AUC reflecting the predictive value of LUS. The AUC was 0.745 (95% CI, 0.606–0.884).

identification of diseased patients and their separation from disease-free patients should be accomplished to reduce the risk of interhuman transmission. However, recent literature[11–16] is also focusing on the role of LUS, but no extensive experiences have been published other than reviews, case reports, small series, and letters to the editor. Conversely, our study aimed to compare these imaging modalities in the detection of COVID-19 disease. Blinded to the results of rRT-PCR testing, LUS and chest CT

examinations were performed, and the specific characteristics of these imaging studies were assessed. The comparison with chest CT was performed to design a proper diagnostic workup according to the general and local technology and human resources.

We have demonstrated that the well-known advantages of LUS in terms of portability and safety were counterbalanced by a sensitivity, specificity, PPV, and NPV of 68%, 79%, 88%, and 52%, respectively, and acceptable diagnostic accuracy. The AUC of LUS summarizes the sufficient/good performance of this tool. Before the outbreak of this new coronavirus, Long et al[17] reported a sensitivity, specificity, and AUC of 88%, 86%, and 0.95 of LUS in detecting pneumonia. Our results, obtained in an emergency setting and with the purpose of rapidly differentiating COVID-19–positive from COVID-19–negative pneumonia, were, obviously, slightly different from that recent systematic review and meta-analysis. On the other hand, chest CT identified patients affected with pneumonia sustained by SARS-CoV-2 infection correctly in 93% of the cases, thus reflecting a low risk of missing infected patients. The specificity was 90%, thus accurately identifying the patients who did not have pneumonia from SARS-CoV-2. The PPV and NPV (85% and 95%) defined the high performance of this diagnostic tool, which was also confirmed by the LR, which was good/excellent. Similarly, the AUC indicated the good/excellent performance of chest CT. Furthermore, the results of both diagnostic tools significantly correlated with symptoms at presentation in COVID-19–positive and COVID-19–negative patients, thus indicating that the severity of the clinical presentation might act as a confounder for diagnosis either in high or low disease prevalence.

Recently, Caruso et al,[18] using rRT-PCR as reference, reported sensitivity of 97%, moderate specificity of 56%, and diagnostic accuracy of 72%. These results were similar to those of Ai et al,[19] who described sensitivity of 97%, specificity of 25%, and accuracy of 68% in patients from Wuhan China. In our study, we observed higher sensitivity and specificity, which were probably related to the improvement of the diagnostic capabilities of our radiologists since the outbreaks in early February. On the other hand, LUS had lower diagnostic accuracy and interobserver agreement because of the intrinsic limits of this diagnostic tool. We are well aware, in fact, that LUS has some specific

limitations that should be seriously considered before recommending widespread use of this tool in the diagnosis of SARS-CoV-2 pneumonia without the support of a confirmatory blood test. A pneumonia location not accessible to US can be, in fact, missed; a patient presenting at a very early stage of lung involvement can be missed; and finally, an eventual overlap with other medical conditions might theoretically give some difficulties in correctly diagnosing COVID-19 in a setting of low disease prevalence.

We had good concordance between the radiologists in diagnosing COVID-19; the κ value showed homogeneity in the evaluation of CT findings between the radiologists, with a discrepancy rate of 6%, corresponding to a disagreement for 1 or 2 features. Conversely, the interobserver agreement of the US operators was acceptable, with a discrepancy rate of 12%, which was related to a disagreement for 1 or 2 features.

In our population, the typical CT features of COVID-19 were a mix between GGO and consolidation areas localized bilaterally in the basal lobes. We also observed bronchiectasis, a thickening of the interlobular septa and the bronchial wall, with an enlargement of the mediastinal lymph nodes. Our findings differed from those of Salehi et al[20] who described a lower presence of consolidations (32%) and a higher presence of GGOs (88%) in a literature review. Similarly, Zhu et al[21] found a higher presence of GGOs (47%) but, similar to our experience, the presence of consolidation (13%). The features of LUS were in some ways comparable to those of chest CT. Particularly, A-lines (indicative of air below the pleural line, corresponding to parietal pleura and expressing a normal US lung aspect) were significantly less represented in COVID-19–positive patients. Conversely, B-lines, which are indicative of diminished lung aeration and give the lung a rocket appearance, were significantly more present in COVID-19–positive compared to COVID-19–negative patients. The presence of a thickened pleural line, bilateralism, and multilobe involvement are the other characteristics of COVID-19–positive patients that may also be found on chest CT. The presence of these features permitted Vetrugno et al[12] to affirm that LUS decreases the use of chest radiography and CT during this pandemic, also making the treatment of these patients more efficient.

Limitations of our study were the relatively small sample size and the inclusion of chest CT and LUS examinations performed only at admission, without including the eventual changes of the disease along with phases of the infection during hospitalization. Furthermore, chest radiography was not performed in all patients, thus not permitting statistical comparisons with that widespread imaging modality. Although there were some weaknesses of our study, some major strengths are represented by the serologic confirmation of the infection by rRT-PCR, the completeness of the preoperative investigations, and the complete follow-up. From a speculative point of view, although we did not investigate the possibility of following the course of the disease the hospitalized patients with LUS, we are confident in recommending this tool because it is radiation free, time saving, and low cost.

In conclusion, our findings demonstrated good reliability of LUS, especially because our intent in the design this study was to validate its role in an emergency setting with patients presenting with different COVID-19 clinical courses. However, since we are well aware of the intrinsic limitations of LUS, especially in a period of low disease prevalence, at present, we are confident in recommending its use in larger clinical trials at universities or highly specialized hospitals supported by confirmatory rRT-PCR and any other tests that would be available and certified.

References

1. Wu Z, McGoogan JM. Characteristics of and important lessons from the coronavirus disease 2019 (COVID-19) outbreak in China: summary of a report of 72,314 cases from the Chinese Center for Disease Control and Prevention [published online ahead of print February 24, 2020]. *JAMA*. https://doi.org/10.1001/jama.2020.2648.

2. Long C, Xu H, Shen Q, et al. Diagnosis of the coronavirus disease (COVID-19): rRT-PCR or CT? *Eur J Radiol* 2020; 126:108961.

3. Fang Y, Zhang H, Xie J, et al. Sensitivity of chest CT for COVID-19: comparison to RT-PCR. *Radiology* 2020; 296:E115–E117.

4. Mayo PH, Copetti R, Feller-Kopman D, et al. Thoracic ultrasonography: a narrative review. *Intensive Care Med* 2019; 45:1200–1211.

5. National Health Commission of the People's Republic of China. Diagnosis and treatment protocol for COVID-19 (trial version 7).

National Health Commission of the People's Republic of China website. http://en.nhc.gov.cn/2020-03/29/c_78469.htm. Accessed June 22, 2020.

6. Ye Z, Zhang Y, Wang Y, Huang Z, Song B. Chest CT manifestations of new coronavirus disease 2019 (COVID-19): a pictorial review. *Eur Radiol* 2020; 30:4381–4389.

7. Soummer A, Perbet S, Brisson H, et al. Lung Ultrasound Study Group. Ultrasound assessment of lung aeration loss during a successful weaning trial predicts post-extubation distress. *Crit Care Med* 2012; 40:2064–2072.

8. Corman VM, Landt O, Kaiser M, et al. Detection of 2019 novel coronavirus (2019-nCoV) by real-time RT-PCR. *Euro Surveill* 2020; 25:2000045.

9. Landis JR, Koch GG. The measurement of observer agreement for categorical data. *Biometrics* 1977; 33:159–174.

10. La Torre M, Mingoli A, Brachini G, et al. Differences between computed tomography and surgical findings in acute complicated diverticulitis. *Asian J Surg* 2020; 43:76–81.

11. Piscaglia F, Stefanini F, Cantisani V, et al. Benefits, open questions and challenges of the use of ultrasound in the COVID-19 pandemic era: the views of a panel of worldwide international experts. *Ultraschall Med* 2020; 41:228–236.

12. Vetrugno L, Bove T, Orso D, et al. Our Italian experience using lung ultrasound for identification, grading and serial follow-up of severity of lung involvement for management of patients with COVID-19. *Echocardiography* 2020; 37:625–627.

13. Soldati G, Smargiassi A, Inchingolo R, et al. Is there a role for lung ultrasound during the COVID-19 pandemic? *J Ultrasound Med* 2020; 39:1459–1462.

14. Lomoro P, Verde F, Zerboni F, et al. COVID-19 pneumonia manifestations at the admission on chest ultrasound, radiographs and CT: single-center study and comprehensive radiologic literature review. *Eur J Radiol Open* 2020; 7:100231.

15. Buonsenso D, Piano A, Raffaelli F, Bonadia N, de Gaetano Donati K, Franceschi F. Point-of-care lung ultrasound findings in novel coronavirus disease-19 pneumoniae: a case report and potential applications during COVID-19 outbreak. *Eur Rev Med Pharmacol Sci* 2020; 24:2776–2780.

16. Peng QY, Wang XT, Zhang LN. Chinese Critical Care Ultrasound Study Group (CCUSG). Findings of lung ultrasonography of novel corona virus pneumonia during the 2019–2020 epidemic. *Intensive Care Med* 2020; 46:849–850.

17. Long L, Zhao HT, Zhang ZY, Wang GY, Zhao HL. Lung ultrasound for the diagnosis of pneumonia in adults: a meta-analysis. *Medicine (Baltimore)* 2017; 96:e5713.

18. Caruso D, Zerunian M, Polici M, et al. Chest CT features of COVID-19 in Rome, Italy. *Radiology* 2020; 296:E79–E85.

19. Ai T, Yang Z, Hou H, et al. Correlation of chest CT and RT-PCR testing in coronavirus disease 2019 (COVID-19) in China: a report of 1014 cases. *Radiology* 2020; 296:E32–E34.

20. Salehi S, Abedi A, Balakrishnan S, Gholamrezanezhad A. Coronavirus disease 2019 (COVID-19): a systematic review of imaging findings in 919 patients. *AJR Am J Roentgenol* 2020; 215:87–93.

21. Zhu W, Xie K, Lu H, Xu L, Zhou S, Fang S. Initial clinical features of suspected coronavirus disease 2019 in two emergency departments outside of Hubei, China [published online ahead of print March 13, 2020]. *J Med Virol*. https://doi.org/10.1002/jmv.25763.